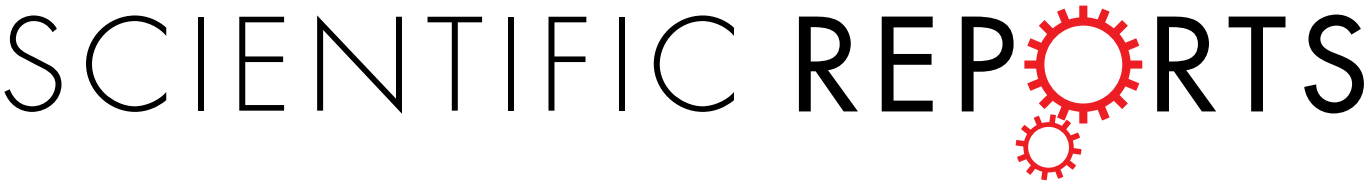

OPEN

Superconductivity of novel tin hydrides (Sn_nH_m) under pressure

M. Mahdi Davari Esfahani[1], Zhenhai Wang[1,2], Artem R. Oganov[1,3,4,5], Huafeng Dong[1], Qiang Zhu[1], Shengnan Wang[1], Maksim S. Rakitin[1] & Xiang-Feng Zhou[1,6]

Received: 03 December 2015
Accepted: 19 February 2016
Published: 11 March 2016

With the motivation of discovering high-temperature superconductors, evolutionary algorithm USPEX is employed to search for all stable compounds in the Sn-H system. In addition to the traditional SnH_4, new hydrides SnH_8, SnH_{12} and SnH_{14} are found to be thermodynamically stable at high pressure. Dynamical stability and superconductivity of tin hydrides are systematically investigated. $I\bar{4}m2$-SnH_8, C2/m-SnH_{12} and C2/m-SnH_{14} exhibit higher superconducting transition temperatures of 81, 93 and 97 K compared to the traditional compound SnH4 with Tc of 52 K at 200 GPa. An interesting bent H_3–group in $I\bar{4}m2$-SnH_8 and novel linear $H\bar{4}$ in C2/m-SnH_{12} are observed. All the new tin hydrides remain metallic over their predicted range of stability. The intermediate-frequency wagging and bending vibrations have more contribution to electron-phonon coupling parameter than high-frequency stretching vibrations of H2 and H3.

Molecular hydrogen's phase transition to a metallic state has been subject of many experimental and theoretical studies[1,2]. Although reaching the metallic state in pure solid hydrogen proved elusive, it is in the main focus of many groups and recently, the progress of bringing pure hydrogen to nearly 400 GPa has been reported[3–5]. Following the pioneering work of Ashcroft[6], nearly room-temperature superconductivity was predicted in metallic molecular hydrogen[7,8].

An alternative approach to metalize hydrogen is to use chemical alloying as a means to exert additional pressure on hydrogen atoms[9]. Hydrogen-rich compounds such as SiH_4 can be metalized at a much lower pressure[10]. For metallic hydrogen, high Debye temperature and strong electron-phonon coupling are anticipated. The same is expected for hydrogen-rich compounds and it has been suggested that hydrogen-rich compounds are good candidates for high-temperature superconductivity[9] Theoretical studies confirm this idea with predicting superconductivity in high-pressure hydrides such as H-Se[11], Ca-H[12], Sn-H[13], Pt-H[14] and B-H[15]. A series of hydrogen-rich compounds have been predicted to have remarkably high T_c values (e.g. 235 K for CaH_6 at 150 GPa[12], 191 K for H_3S at 200 GPa[16], 64 K for GeH_4 at 220 GPa[17]) while the highest T_c that had been achieved experimentally was in the complex mercury cuprate (138 K at ambient pressure[18] and 166 K at high pressures[19]). The new record of high T_c was established for H_3S, a compound whose existence and superconductivity at 200 K were first predicted theoretically[16] in 2014 using USPEX and then observed experimentally[20] in 2015, and started a new wave of interest in hydrogen-rich superconductors.

In a previous theoretical study, Tse *et al.* reported a high-pressure metallic phase of SnH_4 with hexagonal P6/mmm symmetry group, which is a layered structure intercalated with H_2 units, and is a superconductor with Tc close to 80 K at 120 GPa[21]. Later, by using evolutionary algorithm USPEX, Gao *et al.*[13] reported two novel metallic phases of SnH_4 with space groups $P6_3$/mmc and Ama2, which both have hexagonal layers of Sn atoms with semi-molecular H_2 units. The reported stability ranges are 96–180 GPa for Ama2, and above 180 GPa for $P6_3$/mmc; with T_c values of 15–22 K at 120 GPa and 52–62 K at 200 GPa for Ama2 and $P6_3$/mmc, respectively[13].

[1]Department of Geosciences, Center for Materials by Design, and Institute for Advanced Computational Science, State University of New York, Stony Brook, NY 11794-2100, USA. [2]Peter Grunberg Research Center, Nanjing University of Posts and Telecommunications, Nanjing, Jiangsu 210003, China. [3]Skolkovo Institute of Science and Technology, Skolkovo Innovation Center, 3 Nobel St., Moscow 143026, Russia. [4]Department of Problems of Physics and Energetics, Moscow Institute of Physics and Technology, 9 Institutskiy Lane, Dolgoprudny City, Moscow Region 141700, Russia. [5]International Center for Materials Discovery, School of Materials Science and Engineering, Northwestern Polytechnical University, Xi'an, Shaanxi 710072, People's Republic of China. [6]School of Physics and Key Laboratory of Weak-Light Nonlinear Photonics, Nankai University, Tianjin 300071, China. Correspondence and requests for materials should be addressed to A.R.O. (email: artem.oganov@stonybrook.edu)

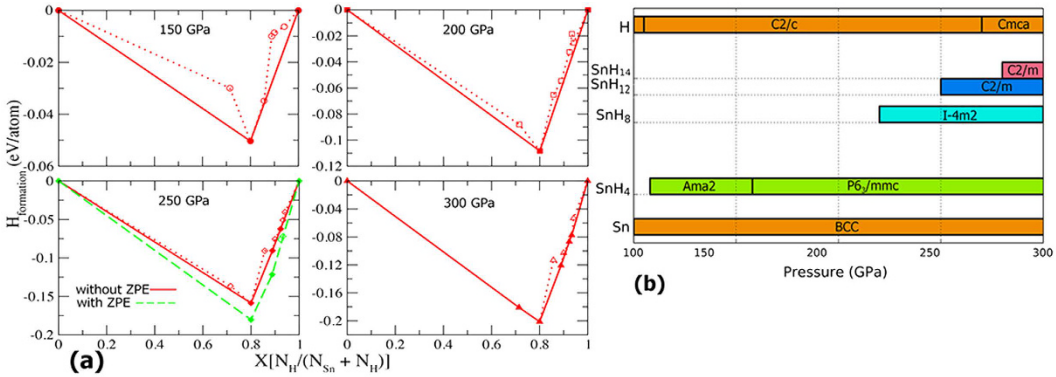

Figure 1. Thermodynamics of the Sn-H system. (**a**) Predicted formation enthalpy of Sn_nH_m compounds. Solid red lines denote the convex hull and green dashed line shows the effect of ZPE inclusion at 250 GPa. (**b**) Predicted pressure-composition phase diagram of the Sn-H system.

While SnH_4 was shown to be a relatively high-T_c superconductor, the possibility of existence of other tin hydrides were not explored so far. At the same time, by now it is proven[22] that totally unexpected compounds become stable under pressure, and this gives hope of finding even better superconductors. Hence, in this study, we systematically search for the stable compounds using the highly efficient variable-composition evolutionary searches (VCES). Apart from the previously reported phases of SnH_4, there is one metastable tetragonal phase of stannane with higher superconducting critical temperature. Other stable superconducting compounds, SnH_8, SnH_{12} and SnH_{14}, are found to become stable at high pressure. Moreover, we found a semi-molecular group H_3– in the $I\bar{4}m2$ structure of SnH_8. Novel H_4–is also present in C2/m-SnH_{12}. We calculate a high T_c of 81 K at 220 GPa in the newly predicted compound SnH_8, 93 K for SnH_{12} at 250 GPa, 97 K for SnH_{14} at 300 GPa and 91 K for the metastable phase of SnH_4 at 220 GPa.

Results

Evolutionary variable-composition searches for stable compounds and their structures with up to 20 atoms in the primitive unit cell were performed at 150, 200, 250 and 300 GPa. To further investigate the newly found compounds, fixed-composition structure predictions for the most promising compounds were performed, with one to three formula units per cell. Candidate low-enthalpy structures are metastable I4/mmm-SnH_4, stable $I\bar{4}$m2-SnH_8, C2/m-SnH_{12} and C2/m-SnH_{14}. In the $I\bar{4}$m2-SnH_8 structure predicted to be stable at pressures above 220 GPa, Sn atoms are packed between H_2 and H_3 molecular groups, in which the bent H_3 units are perpendicular to one another and sepated by 1.35 Å. In C2/m-SnH_{12}, Sn atoms form well-separated close-packed layers intercalated with blocks of H_2 and H_4 semi-molecules.

Figure 1(a). shows the enthalpy of formation (ΔH) of Sn-H compounds at selected pressures. Significantly, in addition to reproducing various structures of solid SnH_4[13,21], Sn[23] and H_2[24], novel compounds SnH_8, SnH_{12} and SnH_{14} are found to be stable in a wide pressure range in our systematic evolutionary structure search. It can be seen from Fig. 1(a). that at around 200 GPa the tetragonal SnH_8 with the space group of $I\bar{4}$m2 lies above the convex hull, therefore, is metastable with respect to decomposition to $P6_3/mmc$-SnH_4 and C2/c-H_2. Between 150 to 300 GPa, we predict stable phases of H_2, SnH_4, SnH_8, SnH_{12}, SnH_{14} and Sn[23]. Some metastable forms of SnH_6, SnH_9 and SnH_{16} are also shown in Fig. 1(a) by open symbols.

SnH_4 is thermodynamically stable at pressures above 108 GPa as was predicted in previous report[13]. It goes through a phase transition at 160 GPa. Upon increasing pressure, at 220 GPa we predict stabilization of SnH_8. SnH_{12} and SnH_{14} reach stability at the pressures of 250 GPa and 280 GPa, respectively, and remain stable at least up to 300 GPa. The structures of SnH_n compounds are found to be dynamically stable within pressure ranges of their stability. In the $I\bar{4}$m2-SnH_8 structure, Sn atoms occupy the 2a Wyckoff site and the H atoms are on the 4e, 8i and 4f sites (detailed structural information is provided in Table 1).

We checked the effects of zero-point energy using phonon calculations[25] at 250 GPa. The inclusion of zero-point noticeably lowered the formation enthalpy of SnH_8 with respect to SnH_4 and H_2 (Fig. 1(a)), implying that this compound can be formed at lower pressure. At the same time, SnH_{12} moves above the convex hull at 250 GPa, suggesting that higher pressure is needed to stabilize C2/m-SnH_{12}. In accord with what we expect, zero-point energy does not change the topology of the phase diagram, but shifts transition pressures.

In $I\bar{4}$m2-SnH_8 structure, the H atoms are split into two categories. Some H atoms form H_3 groups, which were previously observed in solid phases of BaH_6[27], in an unstable structure of H_5Br ($[H_3]Br[H_2]$)[28], and in an intriguing linear form with the bond length of 0.92 Å in H_5Te_2[29]. In contrast to H_5Br, which has approximately an equilateral triangle form of H_3, here we report the formation of H_3 in a bent geometry with the angle of 146.2° and bond length of 0.86 Å at 220 GPa in the $I\bar{4}$m2 structure. The other type of H atoms form H_2 groups which are aligned parallel to each other.

$I\bar{4}$m2 structure can be presented as $Sn[H_2][H_3]_2$ as shown in Fig. 2(a,b). The bond length in H_3 unit is 0.86 Å, whereas H_2 has a longer bond length of 0.87 Å. Contrary to isolated H_2 molecule, which only has a filled σ bonding orbital, in the H_2 and H_3 semi-molecules, population of anti-bonding orbitals causes lengthening and

Phase	Lattice parameters	Atom	x	y	z
$I\bar{4}m2$	a = 3.076 Å	Sn(2a)	0.0000	0.0000	0.0000
SnH_8	c = 5.523 Å	H_1(8i)	0.2729	0.0000	0.3331
	at 220 GPa	H_2(4e)	0.0000	0.0000	0.6208
		H_3(4f)	0.0000	0.5000	0.1701
C2/m	a = 5.191 Å	Sn(2d)	0.0000	0.5000	0.5000
SnH_{12}	b = 3.065 Å	H_1(4i)	0.0495	0.0000	0.6553
	c = 7.388 Å	H_2(4i)	0.4564	0.0000	0.7226
	β = 148.95°	H_3(4i)	0.3428	0.0000	0.8832
	at 250 GPa	H_4(8i)	0.3810	0.2399	0.1123
		H_5(4g)	0.0000	0.1233	0.0000
C2/m	a = 7.129 Å	Sn(2b)	0.0000	0.5000	0.0000
SnH_{14}	b = 2.730 Å	H_1(4i)	0.3651	0.0000	0.7031
	c = 3.673 Å	H_2(4i)	0.1857	0.0000	0.9852
	β = 60.71°	H_3(4i)	0.0732	0.0000	0.6252
		H_4(4i)	0.8063	0.0000	0.8090
	at 300 GPa	H_5(8i)	0.2365	0.2808	0.4035
		H_6(2d)	0.0000	0.5000	0.5000
		H_7(2c)	0.0000	0.0000	0.5000

Table 1. Predicted crystal structures of SnH_8, SnH_{12} and SnH_{14} at 220, 250 and 300 GPa, respectively.

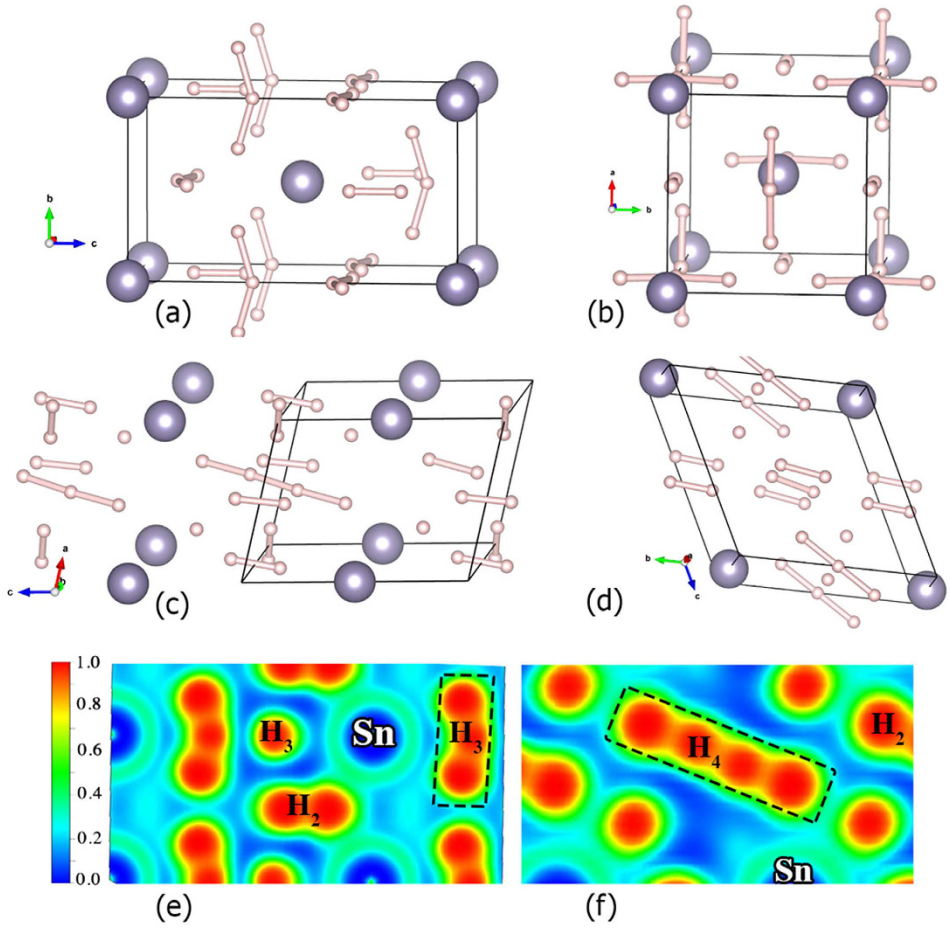

Figure 2. Predicted structures of (**a**,**b**) SnH_8 [$I\bar{4}m2$], (**c**) SnH_{12} [C2/m] and (**d**) SnH_{14} [C2/m]. Large and small spheres represent Sn and H atoms, respectively. Electron localization functions (ELF) for (**e**) SnH_8 [$I\bar{4}m2$] at 220 GPa and (f) SnH_{12} [C2/m] at 250 GPa.

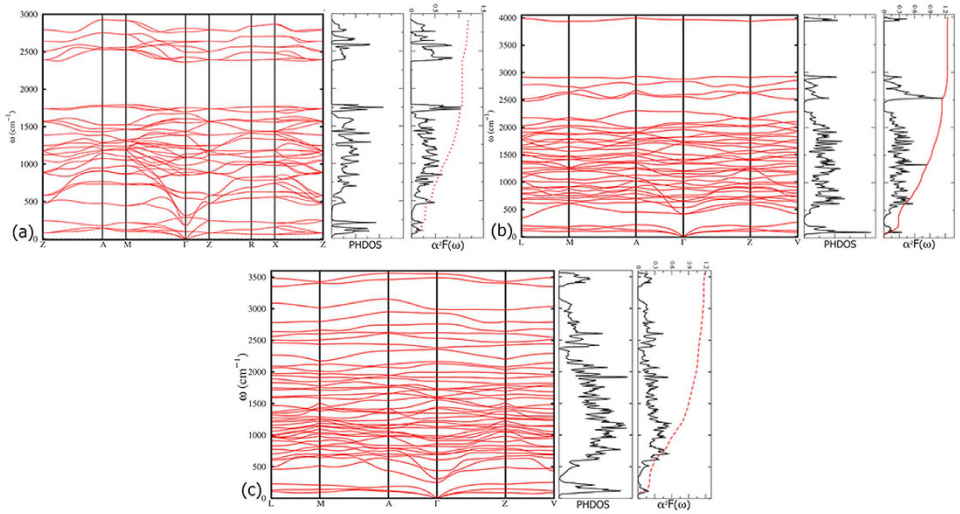

Figure 3. Phonon band structure, phonon DOS, Eliashberg phonon spectral function $\alpha^2F(\omega)$ and electron-phonon integral $\lambda(\omega)$ of: (**a**) SnH_8 [$I\bar{4}m2$] at 220 GPa, (**b**) SnH_{12} [C2/m] at 250 GPa and (**c**) SnH_{14} [C2/m] at 300 GPa.

weakening of the covalent bond. The slightly longer H-H bond length compared to isolated H_2 molecule (0.74 Å) is caused by charge transfer of 0.42 e^- and 0.48 e^-, as computed using Bader theory[26], from Sn to each H_2 and H_3 unit, respectively. Charge transfer is an important factor in the formation of H_2 and H_3 units in the H_4Te, GeH_4, SnH_4, CaH_4, H_5Te_2, H_5Br, BaH_6[12,17,27–29]

Analysis of electron localization function (ELF) shows a high ELF value of 0.88 between H atoms within the unit, indicating strong covalent bonding features (Fig. 2(e)). At the same time, the ELF value on the Sn-H bond is very low, reaching just 0.37.

In C2/m-SnH_{12}, intriguing formation of novel H_4 semi-molecules are observed; at 250 GPa, they can be represented as two H_2-groups separated by just 0.99 Å. Higher pressure of 300 GPa decreases the distance to 0.88 Å, leading to a strong covalent bond in the H_4^- units. Fig. 2(f). demonstrates covalent bonds in the linear H_4 units with the ELF magnitude of 0.85.

The calculated phonon dispersion curves and phonon density of states for $I\bar{4}m2$ structure of SnH_8 at 220 GPa are shown in Fig. 3(a). Dynamical stability is clearly evidenced by the absence of any imaginary frequencies in the whole Brillouin zone. The low-frequency bands below 250 cm^{-1} are mainly from the vibrations of Sn atoms. Modes between 300 and 1700 cm^{-1} are mainly from the H-H wagging vibrations, and higher frequency vibrations above 2300 cm^{-1} are due to H-H stretching vibrations in H_2 and H_3 units.

Low-frequency translational modes, mostly from Sn atom, contribute 23.7% (9.2%) to the total λ. Intermediate H-H wagging vibrations make a significant contribution of 65.7% (67.9%), and the rest is from stretching H vibrations, which contribute 10.6% (22.9%) for SnH_8 (SnH_{12}). This is different from superconductivity in Cmcm-H_2Br[28], where Br translational modes make the largest contribution to the total λ and similar to the $R\bar{3}$ m-H_4Te[29] and P4/mmm-BaH_6[27], where medium-frequency H-wagging and bending modes contribute the most to the EPC. In accord with our expectation, λ increases almost linearly with hydrogen content, where we found 60.2%, 72.2% and 77.1% contribution of H vibrations to the total λ of SnH_4, SnH_8 and SnH_{12}, respectively. This highlights the dominant role of H in the superconductivity of H-rich compounds.

Electronic band structure of $I\bar{4}m2$-SnH_8 is depicted in Fig. 4. Occurrence of flat and steep bands near the Fermi level has been suggested as a condition for enhancing electron-phonon coupling (EPC) and the formation of Cooper pairs.

We can calculate T_c based on the spectral function $\alpha^2F(\omega)$ and taking advantage of Allen-Dynes modified McMillan equation (Eq. 1.) by using Coulomb pseudo-potential μ^* of 0.10 and 0.13 as widely accepted values (see Table 2). At 220 GPa, the predicted T_c values for $I\bar{4}m2$-SnH_8 are 81 K and 72 K using μ^* values of 0.10 and 0.13, respectively. The calculated T_c slightly decreases with pressure (82 K at 200 GPa and 79 K at 300 GPa using $\mu^* = 0.10$) with a pressure coefficient of -0.023 K/GPa $\left(\frac{dT_c}{dP}\right)$. Reported λ is comparable to H_3Se ($\lambda = 1.09$) at 200 GPa[11], but in $I\bar{4}m2$-SnH_8 structure, we have a lower $\langle \omega_{log} \rangle$ of 919 K (1477 K for H_3Se), resulting in a lower T_c value.

In conclusion, we explored the energetically stable/metastable high-pressure phases of the Sn-H system in detail by means of *ab initio* evolutionary structure prediction. The results demonstrate that SnH_8, SnH_{12} and SnH_{14}, reported for the first time in this work, are thermodynamically stable compounds that coexist stably with solid Sn, H_2 and SnH_4 in a wide pressure range starting from 220 to at least 300 GPa.

EPC calculations indicate that high-pressure SnH_8, SnH_{12} and SnH_{14} are phonon-mediated superconductors with T_c values of 81, 93 and 97 K at pressures of 220, 250, and 300 GPa, respectively. λ is high for SnH_n compounds, comparable with H_3M-$Im\bar{3}m$, where M = S and Se[11]. Structures of SnH_n compounds contain H_2^-, bent H_3^-, and linear H_4^- groups. Further experimental studies on the formation of $SnHn$, n = 8, 12 and 14 at high pressure are needed, and present results will serve as a guide for future experiments.

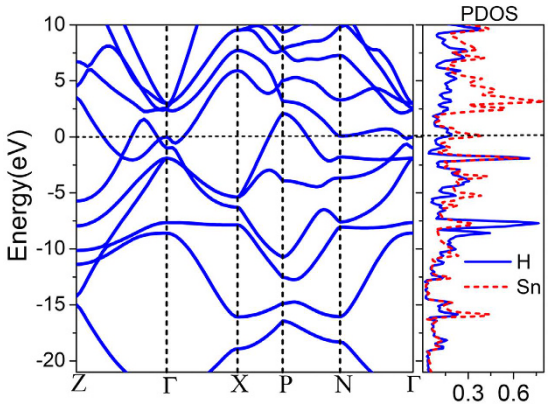

Figure 4. Electronic band structure and projected DOS on Sn and H atoms for SnH_8 [$I\bar{4}m2$] at 220 GPa.

Structure	Pressure (GPa)	λ	ω_{log} (K)	T_c (K)
I4/mmm SnH_4	220	1.180	1025	91 ($\mu^* = 0.10$)
				80 ($\mu^* = 0.13$)
$I\bar{4}m2$-SnH_8	220	1.188	919	81 ($\mu^* = 0.10$)
				72 ($\mu^* = 0.13$)
C2/m-SnH_{12}	250	1.250	991	93 ($\mu^* = 0.10$)
				83 ($\mu^* = 0.13$)
C2/m-SnH_{14}	300	1.187	1099	97 ($\mu^* = 0.10$)
				86 ($\mu^* = 0.13$)

Table 2. The calculated EPC parameter (λ), logarithmic average phonon frequency (ω_{log}) and critical temperature (T_c) (with $\mu^* = 0.10$ and 0.13) for metastable SnH_4, stable SnH_8, SnH_{12} and SnH_{14} at 220, 220, 250 and 300 GPa, respectively.

Methods

To find stable and low-enthalpy metastable structures, we took advantage of evolutionary algorithm implemented in USPEX code[30–32], which has been extensively used to predict stable crystal structures with just a knowledge of the chemical composition and without any experimental information[15,33–35].

In this method, the initial generation of structures and compositions is produced with the random symmetric algorithm[34], and subsequent generations are produced by carefully designed variation operators. In order to find all stable stoichiometric compounds and the corresponding stable and metastable structures in the Sn-H binary system, we used VCES method implemented in USPEX[30,31].

Structure relaxations were carried out using VASP package[36] in the framework of density functional theory (DFT) and using PBE-GGA (Perdew-Burke-Ernzerhof generalized gradient approximation)[37]. The projector-augmented wave approach (PAW)[38] was used to describe the core electrons and their effects on valence orbitals. The plane-wave kinetic energy cutoff was chosen as 1000 eV for hard PAW potentials, and we used Γ-centered uniform *k*-points meshes to sample the Brillouin zone.

Phonons and thermodynamic properties of Sn-H compounds are calculated using the PHONOPY package[25,39]. The supercell approach is used with supercell dimensions greater than 10 Å (typically $3 \times 3 \times 3$ replication of the primitive cell). We used valence electron configurations of $4d^{10}\ 5s^2\ 5p^2$ and $1s^1$ for tin and hydrogen, respectively. Phonon frequencies and electron-phonon coupling (EPC) coefficients are calculated using DFPT as implemented in the Quantum ESPRESSO (QE) code[40]. In the QE calculations, we employed ultrasoft pseudopotentials and PBE-GGA exchange-correlation functional[37]. A plane-wave basis set with a cutoff of 70 Ry gave a convergence in energy with a precision of 1 meV/atom. The EPC parameter was calculated using $4 \times 4 \times 3$, $5 \times 5 \times 4$ and $5 \times 5 \times 4$ *q*-point meshes for $I\bar{4}m2$-SnH_8, C2/m-SnH_{12} and C2/m-SnH_{14}, respectively. Denser *k*-point meshes, $8 \times 8 \times 6$, $10 \times 10 \times 8$ and $10 \times 10 \times 8$ were used for convergence checks for the EPC parameter λ. The superconducting T_c, was estimated using the Allen-Dynes modified McMillan equation[41]:

$$T_c = \frac{\omega_{log}}{1.2} exp\left(\frac{-1.04(1+\lambda)}{\lambda - \mu^*(1+0.62\lambda)}\right) \quad (1)$$

where ω_{log} is the logarithmic average frequency and μ^* is the Coulomb pseudopotential, for which we used 0.10 and 0.13 values, which often give realistic results. The EPC constant and ω_{log} were calculated as:

$$\lambda = 2\int_0^\infty \frac{\alpha^2 F(\omega)}{\omega} d\omega \tag{2}$$

and

$$\omega_{log} = exp\left[\frac{2}{\lambda}\int \frac{d\omega}{\omega}\alpha^2 F(\omega) ln(\omega)\right] \tag{3}$$

References

1. Nellis, W. J. Dynamic compression of materials: metallization of fluid hydrogen at high pressures. *Rep. Prog. Phys.* **69,** 1479 (2006).
2. Loubeyre, P., Occelli, F. & LeToullec, R. Optical studies of solid hydrogen to 320 GPa and evidence for black hydrogen. *Nature* **416,** 613–617 (2002).
3. Zha, C.-S., Liu, Z., Ahart, M., Boehler, R. & Hemley, R. J. High-Pressure Measurements of Hydrogen Phase IV Using Synchrotron Infrared Spectroscopy. *Phys. Rev. Lett.* **110,** 217402 (2013).
4. Howie, R. T., Scheler, T., Guillaume, C. L. & Gregoryanz, E. Proton tunneling in phase IV of hydrogen and deuterium. *Phys. Rev. B* **86,** 214104 (2012).
5. Zha, C.-S., Cohen, R. E., Mao, H.-k. & Hemley, R. J. Raman measurements of phase transitions in dense solid hydrogen and deuterium to 325 GPa. *Proc. Natl. Acad. Sci.* **111,** 4792–4797 (2014).
6. Ashcroft, N. W. Metallic hydrogen: A high-temperature superconductor? *Phys. Rev. Lett.* **21,** 1748–1749 (1968).
7. Cudazzo, P. *et al.* Electron-phonon interaction and superconductivity in metallic molecular hydrogen. II. Superconductivity under pressure. *Phys. Rev. B* **81,** 134506 (2010).
8. Cudazzo, P. *et al.* Electron-phonon interaction and superconductivity in metallic molecular hydrogen. I. Electronic and dynamical properties under pressure. *Phys. Rev. B* **81,** 134505 (2010).
9. Ashcroft, N. W. Hydrogen dominant metallic alloys: High temperature superconductors? *Phys. Rev. Lett.* **92,** 187002 (2004).
10. Eremets, M. I., Trojan, I. A., Medvedev, S. A., Tse, J. S. & Yao, Y. Superconductivity in hydrogen dominant materials: Silane. *Science* **319,** 1506–1509 (2008).
11. Zhang, S. *et al.* Phase Diagram and High-Temperature Superconductivity of Compressed Selenium Hydrides. *ArXiv e-prints* (2015).
12. Wang, H., Tse, J. S., Tanaka, K., Iitaka, T. & Ma, Y. Superconductive sodalite-like clathrate calcium hydride at high pressures. *Proc. Natl. Acad. Sci.* **109,** 6463–6466 (2012).
13. Gao, G. *et al.* High-pressure crystal structures and superconductivity of Stannane (SnH4). *Proc. Natl. Acad. Sci.* **107,** 1317–1320 (2010).
14. Zhou, X.-F. *et al.* Superconducting high-pressure phase of platinum hydride from first principles. *Phys. Rev. B* **84,** 054543 (2011).
15. Hu, C.-H. *et al.* Pressure-Induced Stabilization and Insulator-Superconductor Transition of BH. *Phys. Rev. Lett.* **110,** 165504 (2013).
16. Duan, D. *et al.* Pressure-induced metallization of dense (H2S)2H2 with high-Tc superconductivity. *Sci. Rep.* **4,** 6968 (2014).
17. Gao, G. *et al.* Superconducting high pressure phase of germane. *Phys. Rev. Lett.* **101,** 107002 (2008).
18. Lokshin, K. A. *et al.* Enhancement of T_c in $HgBa_2Ca_2Cu_3O_{8+\delta}$ by fluorination. *Phys. Rev. B* **63,** 064511 (2001).
19. Monteverde, M. *et al.* High-pressure effects in fluorinated $HgBa_2Ca_2Cu_3O_{8+\delta}$. *Europhys. Lett.* **72** , 458 (2005).
20. Drozdov, A. P., Eremets, M. I., Troyan, I. A., Ksenofontov, V. & Shylin, S. I. Conventional superconductivity at 203 kelvin at high pressures in the sulfur hydride system. *Nature* **525,** 73–76 (2015).
21. Tse, J. S., Yao, Y. & Tanaka, K. Novel Superconductivity in Metallic SnH4 under High Pressure. *Phys. Rev. Lett.* **98,** 117004 (2007).
22. Zhang, W. *et al.* Unexpected stable stoichiometries of sodium chlorides. *Science* **342,** 1502–1505 (2013).
23. Giefers, H. *et al.* Phonon Density of States of Metallic Sn at High Pressure. *Phys. Rev. Lett.* **98,** 245502 (2007).
24. Pickard, C. J. & Needs, R. J. Structure of phase III of solid hydrogen. *Nature Phys.* **3,** 473–476 (2007).
25. Togo, A., Oba, F. & Tanaka, I. First-principles calculations of the ferroelastic transition between rutile-type and $CaCl_2$-type SiO_2 at high pressures. *Phys. Rev. B* **78,** 134106 (2008).
26. Bader, R. F. W. *Atoms in Molecules: A Quantum Theory*. Oxford Univ. Press (1990).
27. Hooper, J., Altintas, B., Shamp, A. & Zurek, E. Polyhydrides of the alkaline earth metals: A look at the extremes under pressure. *J. Phys. Chem. C* **117,** 2982–2992 (2013).
28. Duan, D. *et al.* Decomposition of solid hydrogen bromide at high pressure. *ArXiv e-prints* (2015).
29. Zhong, X. *et al.* Tellurium Hydrides at High Pressures: High-temperature Superconductors. *ArXiv e-prints* (2015).
30. Oganov, A. R. & Glass, C. W. Crystal structure prediction using ab initio evolutionary techniques: principles and applications. *J. Chem. Phys* **124** , 244704 (2006).
31. Glass, C.W., Oganov, A.R. & Hansen, N. USPEX-Evolutionary crystal structure prediction. *Comp. Phys. Comm.* **175,** 713–720 (2006).
32. Oganov, A.R., Lyakhov, A.O. & Valle, M. How Evolutionary Crystal Structure Prediction Works-and Why. *Acc. Chem. Res.* **44,** 227–237 (2011).
33. Martinez-Canales, M. *et al.* Novel Structures and Superconductivity of Silane under Pressure. *Phys. Rev. Lett.* **102** (2009).
34. Lyakhov, A.O., Oganov, A. R., Stokes, H.T. & Zhu, Q. New developments in evolutionary structure prediction algorithm USPEX. *Comput. Phys. Commun.* **184,** 1172–1182 (2013).
35. Oganov, A. R. *et al.* Ionic high-pressure form of elemental boron. *Nature* **457,** 863–867 (2009).
36. Kresse, G. & Furthmüller, J. Efficient iterative schemes for *ab initio* total-energy calculations using a plane-wave basis set. *Phys. Rev. B* **54,** 11169–11186 ((1996).
37. Perdew, J. P., Burke, K. & Ernzerhof, M. Generalized gradient approximation made simple. *Phys. Rev. Lett.* **77,** 3865–3868 (1996).
38. Blöchl, P. E. Projector augmented-wave method. *Phys. Rev. B* **50,** 17953–17979 (1994).
39. Togo, A. & Tanaka, I. First principles phonon calculations in materials science. *Scr. Mater.* **108,** 1–5 (2015).
40. Giannozzi, P. *et al.* Quantum espresso: a modular and open-source software project for quantum simulations of materials. *J. Phys. Condens. Matter* **21,** 395502 (2009).
41. Allen, P. B. & Dynes, R.C. Transition temperature of strong-coupled superconductors reanalyzed. *Phys. Rev. B* **12,** 905–922 (1975).

Acknowledgements

We thank DARPA (grant W31P4Q1210008), the Government of Russian Federation (14.A12.31.0003) and the Foreign Talents Introduction and Academic Exchange Program (B08040). X.F.Z thanks the National Science Foundation of China (grant no. 11174152), the National 973 Program of China (grant no. 2012CB921900) and the Program for New Century Excellent Talents in University (grant no. NCET-12-0278). Calculations were mainly performed on the cluster (QSH) in our laboratory at Stony Brook University.

Author Contributions

M.M.D.E. performed all the calculations presented in this article with help from Z.W., Q.Z. and H.D. Research was designed by A.R.O. S.W, M. R. and X-F. Z. analyzed data. M.M.D.E., A.R.O. and Z.W. wrote the first draft of the paper and all authors contributed to revisions.

Additional Information

Competing financial interests: The authors declare no competing financial interests.

How to cite this article: Mahdi Davari Esfahani, M. *et al.* Superconductivity of novel tin hydrides (Sn_nH_m) under pressure. *Sci. Rep.* **6**, 22873; doi: 10.1038/srep22873 (2016).